Dexmedetomidine exerts cardioprotective effect through miR-146a-3p targeting *IRAK1* and *TRAF6* via inhibition of the NF-κB pathway

Liang He[a,b,1], Zhuoran Wang[a,1], Rui Zhou[a,1], Wei Xiong[a], Yuqiao Yang[a], Ning Song[a], Jinqiao Qian[a,*]

[a] *Department of Anesthesiology, First Affiliated Hospital of Kunming Medical University, Kunming, Yunnan Province, 650032, China* [b] *Department of Anesthesiology, Yan'an Hospital of Kunming City, Kunming Medical University, Kunming, Yunnan Province, 650051, China*

ARTICLEINFO

Keywords:
Dexmedetomidine miR-146a-3p
ROS
IRAK1
TRAF6
NF-κB pathway

ABSTRACT

Background: Myocardial ischemia/reperfusion (I/R) injury is a common cause of mortality. Cardiac miR-146a is emerging as a potent regulator of myocardial function. Dexmedetomidine preconditioning provides cardioprotective effects, of which mechanisms related to miR-146a-3p are unclear.

Methods: A myocardial I/R model in rats and a cellular anoxia/reoxygenation (A/R) model in H9C2 cells were established and preconditioned with dexmedetomidine or not. H9C2 cells were transfected with mimics, inhibitor, or negative controls of miR-146a-3p, and siRNAs of *IRAK1* or *TRAF6*. Relative expressions of miR-146a- 3p were determined by quantitative real-time polymerase chain reaction. The apoptosis rates and reactive oxygen species (ROS) levels in H9C2 cells were examined by flow cytometry. Protein expressions of IRAK1, TRAF6, cleaved Caspase-3, BAX, BCL-2, NF-κB p65, phosphorylated NF-κB p65 (p-NF-κB p65), IκBα, and phosphorylated IκBα (p-IκBα) in H9C2 cells were detected by Western blot.

Results: Dexmedetomidine decreased myocardial infarction size and apoptosis rates of H9C2 cells. Dexmedetomidine upregulated expression of miR-146a-3p. Dexmedetomidine significantly decreased protein expressions of IRAK1, TRAF6, cleaved Caspase-3, BAX, and NF-κB p65, but increased expressions of BCL-2 in H9C2 cells. miR- 146a-3p overexpression strengthened the anti-apoptotic effect induced by dexmedetomidine in H9C2 cells *via* decreasing protein levels of IRAK1, TRAF6, cleaved Caspase-3, BAX, NF-κB p65, p-NF-κB p65, and p-IκBα and increasing protein level of BCL-2. Downregulation of miR-146a-3p reversed the changes in these proteins in H9C2 cells. Expressions of NF-κB p65 and p-NF-κB p65 were further decreased following knockdown of *IRAK1* or *TRAF6*. ROS emission was significantly increased after A/R, while significantly decreased following dexmedetomidine preconditioning in H9C2 cells transfected with siIRAK1 or siTRAF6.

Conclusion: miR-146a-3p targeting *IRAK1* and *TRAF6* through inhibition of NF-κB signaling pathway and ROS emission is involved in cardioprotection induced by dexmedetomidine pretreatment.

1. Introduction

In an updated statistical analysis of diseases, myocardial infarction measures can also result in ischemia/reperfusion injury (IRI) [4], which (MI) remains the leading cause of death and disability worldwide [1]. may contribute to reperfusion arrhythmia and myocardial dysfunction

Reperfusion therapies including thrombolysis, percutaneous coronary [5,6]. Furthermore, perioperative myocardial injury including MI may intervention, and coronary artery bypass grafting are the most effective strategies against acute MI [2,3]. However, these effective reperfusion

Abbreviations: A/R, anoxia/reoxygenation; BCL-2, B-cell lymphoma-2; CCK-8, cell counting kit-8; CON, control; DEX, dexmedetomidine; DHE, dihydroethidium; DP, dexmedetomidine preconditioning; Inh, miR-146a-3p inhibitor; IRAK1, interleukin-1 receptor-associated kinase 1; I/R, ischemia/reperfusion; IRI, ischemia/ reperfusion injury; LAD, left anterior descending; MI, myocardial infarction; Mim, miR-146a-3p mimic; miR(s), microRNA(s); NC, negative control; qRT-PCR, quantitative real-time polymerase chain reaction; rIJV, right internal jugular vein; ROS, reactive oxygen species; TRAF6, tumor necrosis factor receptor-associated factor 6; TTC, 2,3,5-triphenyltetrazolium chloride.

* Corresponding author at: Department of Anesthesiology, First Affiliated Hospital of Kunming Medical University, #295 Xichang Road, Kunming, Yunnan Province, 650032, China.

E-mail address: qianjinqiao@126.com (J. Qian).

[1] These authors contributed equally to this work.

https://doi.org/10.1016/j.biopha.2020.110993
Received 8 June 2020; Received in revised form 28 October 2020; Accepted 1 November 2020
Available online 18 November 2020
0753-3322/© 2020 The Authors. Published by Elsevier Masson SAS. This is an open access article under the CC BY-NC-ND license (http://creativecommons.org/licenses/by-nc-nd/4.0/).

cause much higher morbidity and mortality than that directly caused by anesthesia itself [7]. Therefore, novel targets for perioperative cardioprotection are warranted.

Dexmedetomidine (DEX), a highly selective α_2-adrenoceptor agonist, has sedative, analgesic, and opioid-sparing effects [8]. Recent studies have indicated that DEX is a potential protective agent against IRI in heart [9–11], brain [12,13] and lung [14]. However, mechanisms of microRNAs (miRs) underlying DEX induced cardioprotection are not completely understood. microRNAs (miRs) are small and single-stranded RNAs consisting of ~22 nucleotides, acting as negative regulators of target genes by inhibiting translation of messenger RNAs (mRNAs) or promoting mRNAs degradation [15,16]. Some miRs are involved in myocardial contraction, electrical signal conduction, development and morphogenesis of heart, and pathogenesis of cardiovascular diseases [11,17,18]. The novel roles of miRs in the cardioprotective effects induced by DEX may provide a possible therapeutic strategy against myocardial IRI.

Upregulation of miR-146a attenuates myocardial IRI [19]. Higher levels of circulating miR-146a are employed to predict left ventricular remodeling after MI [20]. miR-146a may serve as a potential biomarker of prognosis for patients with atrial fibrillation [21] and a therapeutic target for peripartum cardiomyopathy [22]. miR-146a may target interleukin-1 receptor-associated kinase 1 (*IRAK1*) and tumor necrosis factor receptor-associated factor 6 (*TRAF6*) [23–26], which prevent cardiomyocytes from apoptosis induced by ischemia or sepsis [27,28]. I/R may result in phosphorylation of IκBα, dissociation of IκBα/NF-κB complex, and translocation of NF-κB to nucleus [29]. And NF-κB signaling pathway is involved in miR-146 against apoptosis of H9C2 cells undergoing oxygen-glucose deprivation [30].

We predicated *IRAK1* and *TRAF6* to be target genes and NF-κB to be the signaling pathway of miR-146a-3p in DEX induced cardioprotection. We hypothesized that DEX preconditioning may induce cardioprotection *via* miR-146a-3p targeting IRAK1/TRAF6/NF-κB axis. The current study was designed to check cardioprotective effect and reveal the underlying mechanisms of cardioprotection.

2. Materials and methods

2.1. Myocardial I/R in rat

The animal study was conducted and approved by recommendations of the Ethics Committee of Kunming Medical University. Thirty-nine male SD rats weighing 260–320 g were included in the study under induction of ether and maintenance with chloral hydrate. After anesthesia, electrocardiography was performed on all rats, which were intubated with a cannula and connected to a rodent ventilator. Volume-controlled ventilation was conducted with a tidal volume of 10 mL / kg at a respiratory rate of 40 breaths / min during the procedures, and body temperature was maintained at about 37 °C. As previously described [31], the right internal jugular vein (rIJV) was isolated for drug administration; after cardiac function stabilization for 15 min under a left thoracotomy, a bolus of heparin (100 U / kg body weight) was administrated through rIJV; occlusion and reperfusion of the left anterior descending (LAD) coronary artery with a prolene ligature was conducted to induce I/R. Rats in the Sham group were blood perfused for 180 min; in the IR group, 30 min of occlusion followed by 120 min of reperfusion of the LAD coronary artery; in the DEX preconditioning (DP) group, DEX (20 μg/kg) was given *via* the rIJV 15 min before I/R. At the end of observation, the hearts were harvested for examination and profiling of miRs using microarray analysis. The expressions of the target miRs were validated by quantitative real-time PCR (qRT-PCR).

2.2. Infarction size

After removal from the heart, the left ventricle was frozen in liquid nitrogen for about 10 s and cut into 2-mm thin slices, which were stained with 1% (w/v) 2,3,5-triphenyltetrazolium chloride (TTC) (Sigma Chemical, Balcatta, USA) for 15 min at 37 °C in the dark. Infarction size was expressed as the percentage of risk area (infarction area of TTC- positive staining, and the similar risk regions among the different groups) of the complete ventricular tissue, according to a previous study [32].

2.3. H9C2 cells culture

Heart-derived H9C2 cells (Chinese Academy of Science Cell Bank, Shanghai, China) were cultured with Dulbecco's modified Eagle's medium (DMEM, Gibco, NY, USA) supplemented with 10 % fetal bovine serum and 1% penicillin-streptomycin solution in humidified air (5% CO_2) at 37 °C. Media were refreshed every 2 days and replaced with a minimal essential serum-free medium for 12 h before drug treatment.

2.4. Cellular A/R model and DEX pretreatment

H9C2 cells were divided into three groups: control (CON), anoxia/ reoxygenation (A/R), and dexmedetomidine (DEX) + A/R. In group CON, H9C2 cells were incubated with normoxia (95 % O_2 and 5% CO_2) at 37 °C for 5 h. A cellular A/R model was established in an anoxic chamber saturated with 1% O_2, 5% CO_2 and 94 % N_2 at 37 °C for 3 h, and then normoxia at 37 °C for 2 h for reoxygenation. In group DEX +A/ R, H9C2 cells were pretreated with 10 nM DEX for 1 h (based upon our previous study [11]) before A/R.

2.5. Luciferase reporter assay

293 T cells were cotransfected with 100 ng firefly luciferase reporter vector with the sequence of wild type (WT) of IRAK1 (or TRAF6) 3′UTR and miR-146a-3p mimics (100 ng), or the predicted binding site in 3′UTR of IRAK1 (or TRAF6) replaced by mutant type (Mut) and miR146a-3p mimics negative control (100 ng), and 5 ng Renilla (a normalization control). Relative luciferase activities normalized by Renilla were measured by a dual-luciferase reporter assay system (Promega, USA) at 48 h after cotransfection.

2.6. H9C2 cells transfection

H9C2 cells were transfected with miR-146a-3p mimics, inhibitor, or negative control (NC) for 48 h using Lipofectamine 2000 (Invitrogen, Carlsbad, USA), according to the manufacturer's instructions. Also, H9C2 cells were transfected with *IRAK1*-siRNAs or *TRAF6*-siRNAs for 24 h using Lipofectamine™ 2000.

2.7. CCK-8 assay

Cell proliferation was detected by cell counting kit-8 (CCK-8) (Beyotime, Nanjing, China) assays. All cultured cells in each well of a 96- hole deep pore plate were incubated with 10 μL of CCK-8 tetrazolium salt at 37 °C for 4 h, and the absorbance was detected by a microplate spectrofluorometer (BioTek Instruments, Inc., Winooski, VT, USA) at a 450 nm wavelength.

2.8. Flow cytometry for detection of apoptotic cells

Flow cytometry was performed to analyze apoptosis rates of H9C2 cells by Annexin V-FITC staining. Briefly, the treated cells were washed with PBS twice, and concentration was adjusted to 5×10^5 cells/mL. Then, 100 μl of the sample (5×10^4 cells) was transferred to a 5-ml culture tube, and 5 μL of Annexin V-FITC and 5 μL of propidium iodide (PI) were added. The cells were gently vortexed and incubated at 25 °C for 15 min in the dark. A total of 500 μL of 1× binding buffer was added to each tube. The cells were analyzed by flow

cytometry (Beckman Coulter CytoFLEX, Indianapolis, IN, USA) immediately.

2.9. DHE staining for determining reactive oxygen species (ROS)

According to previous study [33], total O_2^- production in H9C2 cells was determined by dihydroethidium (DHE) staining (Beyotime, China). DHE is oxidized by intracellular O_2^- and then it combines with the chromosomal DNA in the nucleus to generate red fluorescence. H9C2 cells treated with 0.25 % trypsin were washed twice with PBS. The washed cells were incubated with 10 μM DHE diluted in 1 mL serum-free DMEM without light at 37 °C. H9C2 cells were washed three times again with 2 mL PBS after 20 min incubation and then fluorescence intensity was determined by flow cytometry. The ratio of fluorescence intensity to the basal level (in Control group) was quantified and regarded as the cellular ROS level.

2.10. Quantitative real-time polymerase chain reaction

Total RNA was isolated from cardiomyocytes using Trizol reagent (Invitrogen, Carlsbad, CA, USA) and was reverse-transcribed to cDNA. Concentration and purity of the extracted total RNA was quantified by an ultraviolet spectrophotometer (Nano-100; Hangzhou, China). High-quality RNA presented an A260/A280 ratio of 1.8 to 2.0. Total RNA was reverse-transcribed in a 20 μL mixture containing 5 μg of total RNA at 25 °C for 5 min, 50 °C for 15 min, 85 °C for 5 min, and 4 °C for 10 min. Quantitative real-time polymerase chain reaction (qRT-PCR) was performed in triplicate using a real-time PCR system (ABI QuantStudio™, Carlsbad, CA, USA), and U6 (as an internal control). Ct values of miR- 146a-3p were normalized by subtracting the U6 Ct value, followed by calculation of the relative expression level between groups using the $2^{-\Delta\Delta Ct}$ method [27,34]. The primers for amplification were as follows: miR-146a-3p, forward: 5′-TGCGCACCTGTGAAGTTCAGT-3′; reverse: 5′-CCAGTGCAGGGTCCGAGGTATT-3′; U6, forward: 5′-CGCTTCGGCAGCACATATAC-3′; reverse: 5′-AAATATGGAACGCTTCACGA-3′.

2.11. Western blot analysis

Total proteins in H9C2 cells were extracted and determined by Western blot analysis. Western blot analyses was conducted using primary antibodies: anti-TRAF6 antibody (diluted 1:2000; Abcam, Cambridge, MA, USA), anti-IRAK1 antibody (diluted 1:1000; Abcam), anti- cleaved capase-3 antibody (diluted 1:2000; Abcam), anti-BAX antibody (diluted 1:1000; Abcam), anti-BCL-2 antibody (diluted 1:1000; Abcam), anti-NF-κB p65 antibody (diluted 1:1000; Proteintech) or anti-phosphorylated NF-κB p65 antibody (p-NF-κB p65, diluted 1:1000; Affinity, Australia), anti-IκBα antibody (diluted 1:1000; Abcam) or anti- phosphorylated IκBα antibody (p-IκBα, diluted 1:1000; Abcam), and anti-GAPDH antibody (1:1000; Boster, Wuhan, China) was used as the loading control. The blots were visualized with enhanced chemiluminescence and quantified by densitometry.

2.12. Statistical analysis

Data are expressed as mean ± standard deviation (SD) of at least three independent experiments for each group. All statistical tests were implemented with SPSS vision 20.0 (IBM). The data were evaluated using Student's *t*-test for comparisons between two groups. One-way analysis of variance was used for multiple comparisons. A *P*-value less than 0.05 was considered significant.

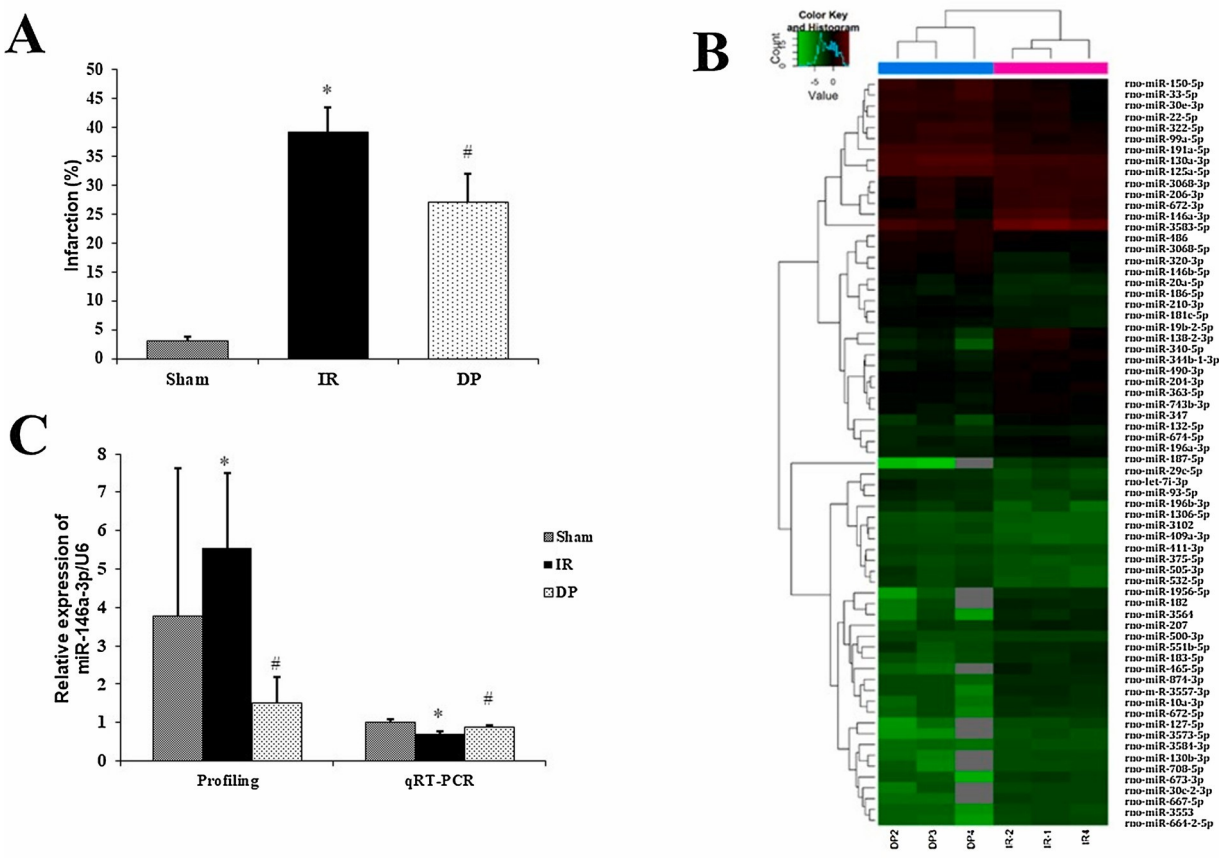

Fig. 1. Effects of DEX on myocardial infarction and expression of miR-146a-3p *in vivo*.
(A) DEX preconditioning (DP) reduced myocardial infarction size (N = 5 in each group). Effects of DEX preconditioning on the expression profiling of miRs (B, C) (N = 3 in each group). Relative expression levels of miR-146a-3p (C) (N = 3 in each group). I/R, ischemia/reperfusion; DEX, dexmedetomidine; DP, DEX preconditioning. qRT-PCR, quantitative real-time polymerase chain reaction. $*P < 0.05$, *versus* Sham group; $^{\#}P < 0.05$, *versus* I/R group.

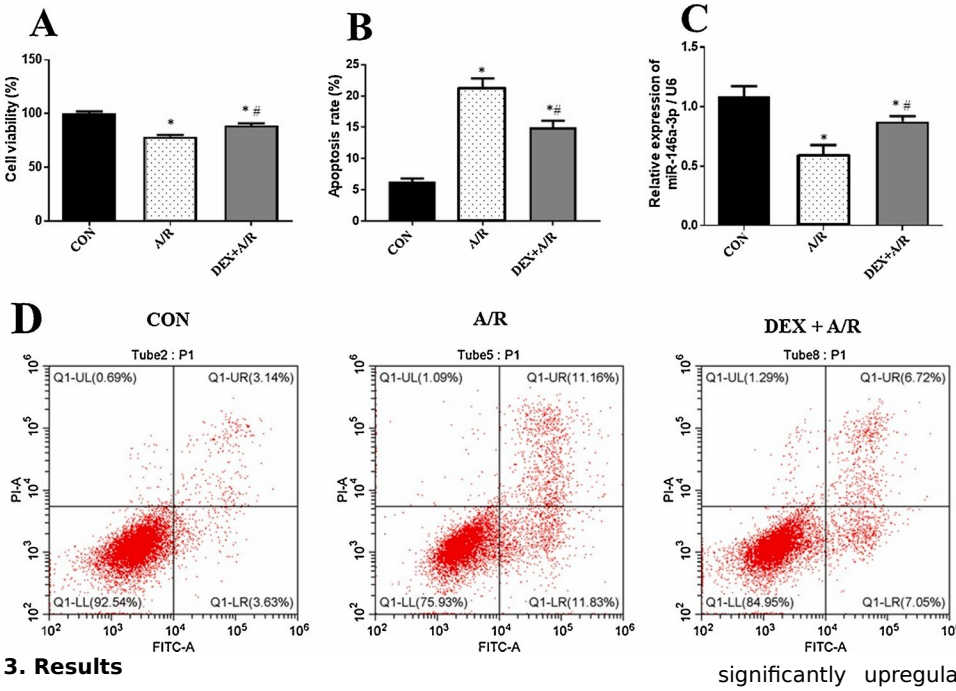

Fig. 2. Effects of DEX on A/R injury and expression of miR-146a-3p. (A) Cell viability, (B) Apoptosis rates, (C) Relative expression of miR-146a-3p, and (D) Flow cytometry analysis were presented in groups CON, A/R, and DEX + A/R. Expression of U6 was used as an internal control. A/R, anoxia/reoxygenation; CON, Control; DEX, dexmedetomidine. N = 3 samples for each group. $*P < 0.05$, *versus* CON group; $^{\#}P < 0.05$, *versus* A/R group.

3. Results

3.1. Effects of DEX on myocardial infarction and expression of miR-146a-3p in vivo

Infarction sizes in rat hearts subjected to I/R were significantly increased compared to those in group Sham, but were significantly decreased in group DP+I/R (Fig. 1A). Profiling of miRs indicated that a total of 83 miRNAs (79 miRNAs in Group IR, and 74 miRNAs in Group DP) were differentially expressed. Compared to those in groups pretreated with DP, a total of 30 miRs (including miR-146a-3p) were significantly upregulated, and 29 miRs downregulated in group IR (Fig. 1B). In miRs profiling, expression of miR-146a-3p in rat hearts pretreated with DEX was significantly

decreased compared with I/R. However, miR-146a-3p was increased in a validation study using qRT- PCR (Fig. 1C).

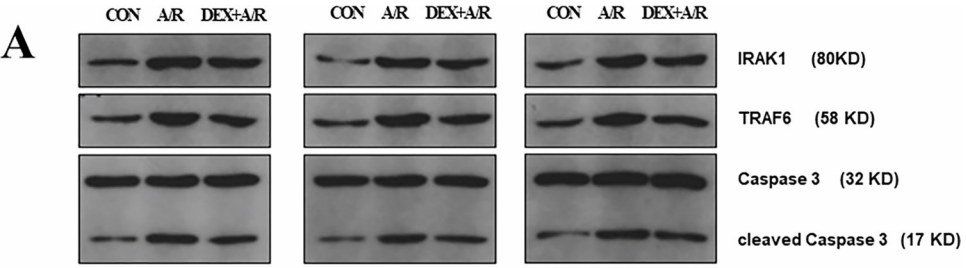

Fig. 3. Effects of DEX on IRAK1, TRAF6, and apoptosis-related proteins of H9C2 cells under A/R.
(A) and (B) Protein levels of IRAK1, TARF6, Caspase-3, cleaved Caspase-3, BAX, and BCL-2 were displayed by western blot analysis in groups CON, A/R, and DEX + A/R. Expression of GAPDH was used as an internal control. A/R, anoxia/reoxygenation; CON, Control; DEX, dexmedetomidine; kD, kilodalton. N = 5 samples for each group. $*P < 0.05$, *versus* Con; $^{\#}P < 0.05$, *versus* A/R.

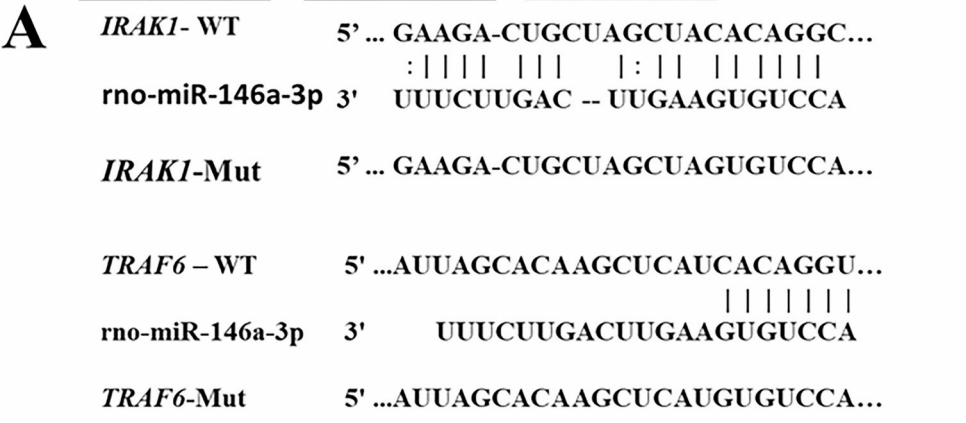

Fig. 4. *IRAK1* and *TRAF6* are target genes of miR-146a-3p.
(A) Predicted target sequences in *IRAK1* or *TRAF6* 3′UTR which can directly bind with miR-146a-3p. (B) Luciferase reporter assay indicates that miR-146a-3p could directly bind with *IRAK1* or *TRAF6*. (C) Sequences. Mim, miR-146a-3p mimics; Mut, mutant type; NC, microRNA-146a-3p mimics negative control; WT, wild type. N = 3 samples for each group. *P < 0.001, *versus* miR-NC + IRAK1; $^{\#}P < 0.001$, *versus* miR-NC + TRAF6.

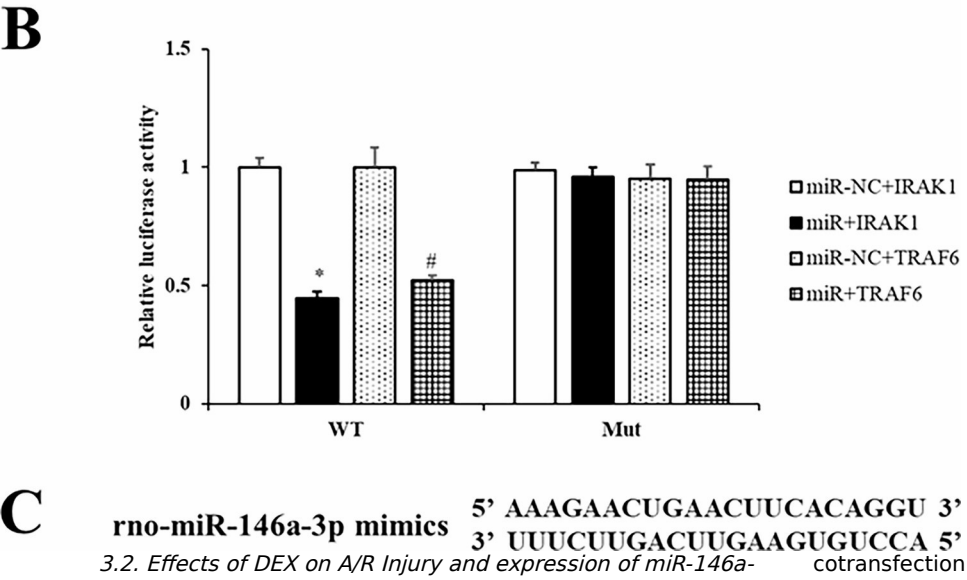

3.2. Effects of DEX on A/R Injury and expression of miR-146a-3p in H9C2 cells

We first examined proliferation and apoptosis rates of the cells subjected to anoxia/reoxygenation (A/R) and the relative expression of miR-146a-3p. Compared with control (CON) group, the viability was significantly decreased in H9C2 under A/R (Fig. 2A), and the apoptotic rates in H9C2 cells weresignificantly increased (Fig. 2B). Then, the protective effect of pretreatment with DEX against A/R injury was determined by observing cell proliferation, apoptosis rates, and expression of miR-146a-3p. DEX increased cell viability, which was decreased in group A/R (Fig. 2A). The expression of miR-146a-3p was significantly decreased in A/R group compared with group CON, while it was significantly increased in DEX + A/R group compared with A/R (Fig. 2C). The apoptotic rates were significantly increased in A/R group compared with CON, while it was significantly decreased in H9C2 cells pretreated with DEX (Fig. 2B, D).

3.3. Effects of DEX on IRAK1, TRAF6, and apoptosis-related proteins of H9C2 cells under A/R

levels of IRAK1 and TRAF6, cleaved caspase-3, and BAX (apoptotic proteins) were significantly increased, while BCL-2 (anti-apoptotic protein) decreased in A/R group compared with CON (Fig. 3A, B). Levels of proteins IRAK1, TRAF6, cleaved caspase-3, and BAX were significantly decreased in DEX + A/R group compared with A/R (Fig. 3A, B).

3.4. Target genes IRAK1 and TRAF6 validated by the luciferase assay report

After searching on miRbase, we found that miR-146a-3p could bind respectively with continuous 6 and 7 bases existing in 3′UTR of *IRAK1* and *TRAF6* (Fig. 4A). Luciferase reporter assay results indicated that the luciferase activity was significantly decreased by cotransfection of miR- 146a-3p mimics with *IRAK1* or *TRAF6* compared to cotransfection of negative control with *IRAK1* or *TRAF6* ($P < 0.001$, Fig. 4B), validating *IRAK1* and *TRAF6* to be target genes of miR-146a-3p.

3.5. Effects of overexpression of miR-146a-3p on apoptosis induced by A/R

According to the flow cytometry results, as shown in Fig. 2B, the apoptotic rates of H9C2 cells were increased in A/R

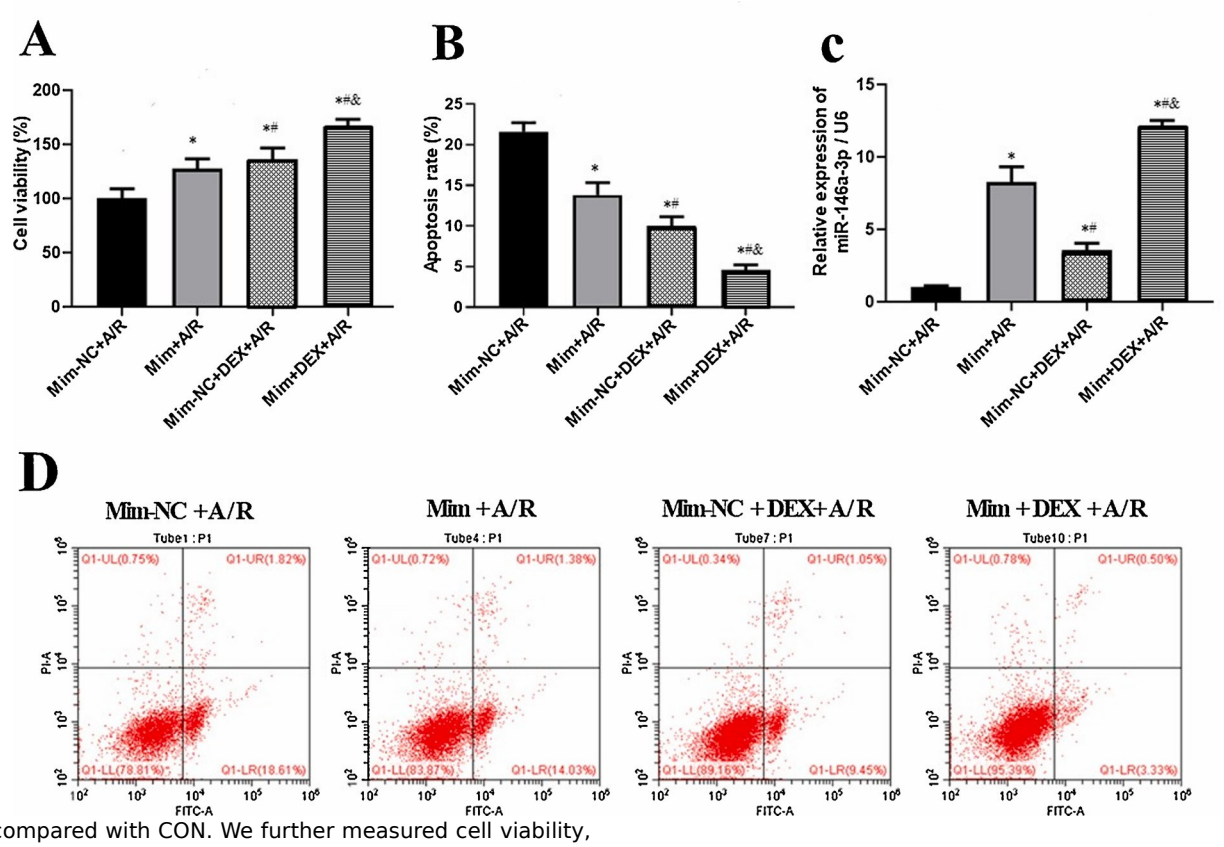

group compared with CON. We further measured cell viability, apoptotic rates, and relative expression of miR-146a-3p in H9C2 cells transfected with miR- 146a-3p mimics (Mim) or its negative control (NC) before A/R. As shown in Fig. 5A–D, miR-146a-3p mimics significantly increased H9C2 cell viability and relative expression of miR-146a-3p after A/R, while apoptotic rates were significantly decreased in group Mim + A/R compared with group Mim-NC + A/R, in group Mim + DEX + A/R compared with group Mim-NC + DEX + A/R, and in group Mim + DEX + A/R compared with group Mim + A/R as well.

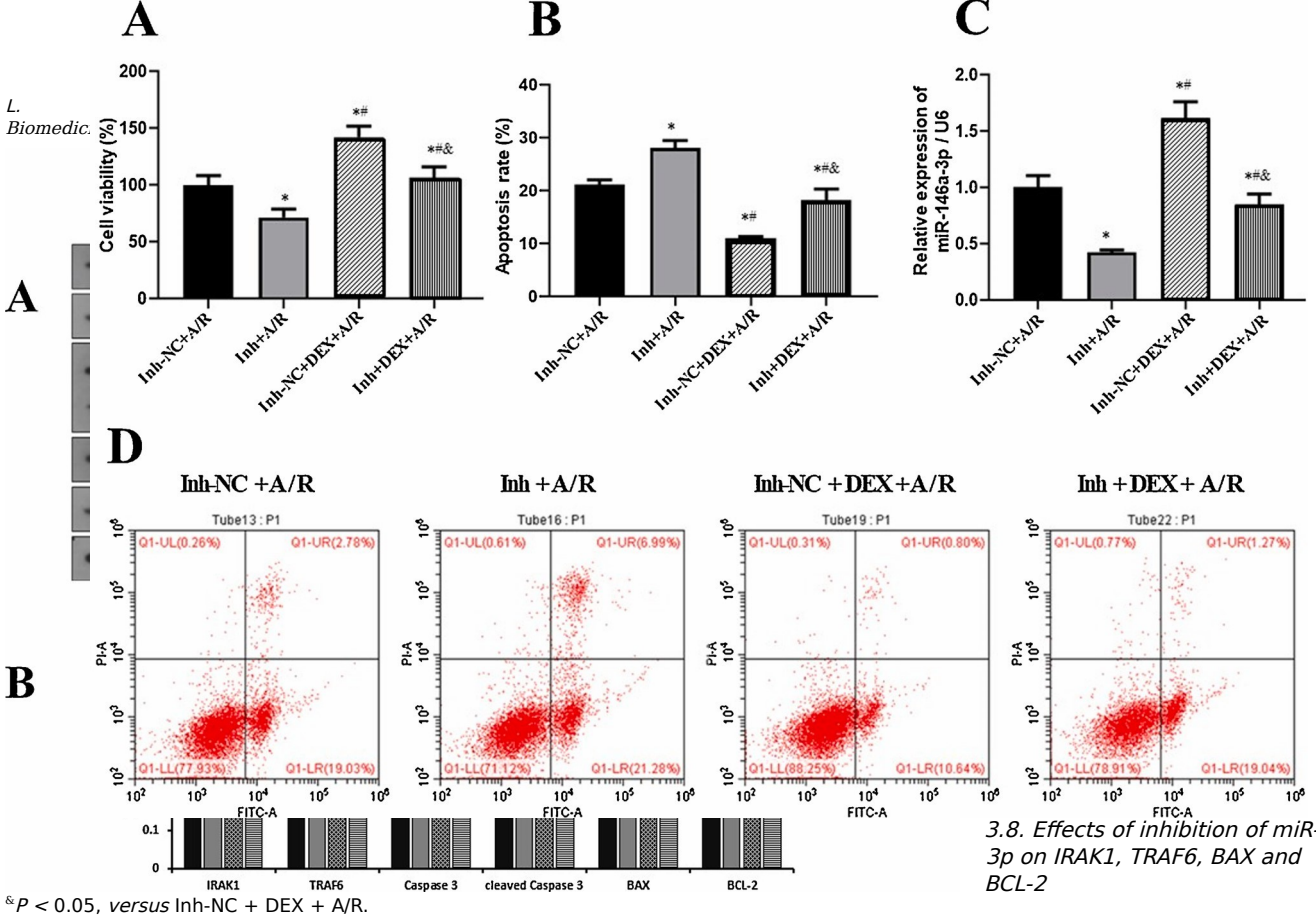

3.8. Effects of inhibition of miR-146a-3p on IRAK1, TRAF6, BAX and BCL-2

[&]$P < 0.05$, *versus* Inh-NC + DEX + A/R.

3.6. Effects of overexpression of miR-146a-3p on IRAK1, TRAF6, BAX, and BCL-2

As shown in Fig. 6A and B, miR-146a-3p mimics dramatically reduced levels of proteins IRAK1, TRAF6, BAX, and cleaved-Caspase-3 in H9C2 cells in group Mim + A/R compared with group Mim-NC + A/R, in group Mim + DEX + A/R compared with group Mim-NC + DEX + A/ R, and in group Mim + DEX + A/R compared with group Mim + A/R as well. However, the protein level of BCL-2 was significantly increased in group Mim + A/R compared with group Mim-NC + A/R, in group Mim + DEX + A/R compared with group Mim-NC + DEX + A/R, and in Mim + DEX + A/R compared with group Mim + A/R. There was no significant difference in expression of Caspase-3 in H9C2 cells in any of the groups.

3.7. Effects of inhibition of miR-146a-3p on apoptosis and viability

As shown in Fig. 7A–D, H9C2 cells transfected with miR-146a-3p inhibitor (Inh) or its negative control (NC) in the presence or absence of DEX were subjected to A/R injury. miR-146a-3p inhibitor (Inh) significantly reduced cell viability, and increased apoptosis rates of H9C2 cells in group Inh + A/R compared with group Inh-NC + A/R, and in group Inh + DEX + A/R compared with group Inh-NC + DEX + A/R. Meanwhile, the relative expression level of miR-146a-3p and cell viability were significantly decreased in group Inh + A/R compared with group Inh-NC + A/R and in group Inh + DEX + A/R compared with group Inh-NC + DEX + A/R. Interestingly, the apoptosis rates of H9C2 cells were decreased in group Inh + DEX + A/R compared with group Inh + A/R (Fig. 7B). The cell viability and the relative expression levels of miR-146a-3p were significantly increased in group Inh + DEX + A/R compared with group Inh + A/R (Fig. 7C).

As shown in Fig. 8A and B, under A/R injury, miR-146a-3p inhibitor dramatically upregulated the protein levels of IRAK1, TRAF6, BAX, and cleaved-Caspase-3 in H9C2 cells in Inh + A/R group compared with Inh-
NC + A/R, and also in Inh + DEX + A/R group compared with Inh-NC + DEX + A/R. Meanwhile, expression of BCL-2 was significantly decreased in Inh + A/R group compared with Inh-NC + A/R, and also in Inh + DEX + A/R group compared with Inh-NC + DEX + A/R. DEX significantly decreased the levels of IRAK1, TRAF6, and cleaved-Caspase-3 in H9C2 cells in Inh + DEX + A/R group compared with Inh + A/R, while level of BCL-2 was significantly increased in Inh + DEX + A/R group compared with Inh + A/R. There was no significant difference in level of Caspase-3 in any of the groups.

3.9. Effects of siIRAK1 or siTRAF6 on NF-κB pathway

H9C2 cells were transfected with *IRAK1*-siRNA or *TRAF6*-siRNA sequences (Fig. 9A). Levels of IRAK1 and TRAF6 in H9C2 cells were increased in group A/R compared with group Control. DEX preconditioning reversed the expression levels of IRAK1 and TRAF6 caused by A/R in H9C2 cells. The protein levels of IRAK1 and TRAF6 in group Mim + DEX + A/R were lower than those in group Mim-NC + DEX + A/
R. The protein levels of IRAK1 and TRAF6 in group Mim + siIRAK1 + DEX + A/R or Mim + siTRAF6 + DEX + A/R were lower than those in group Mim-NC + DEX + A/R (Fig. 9B, C). Expressions of p-IκBα, NF-κB p65, and p-NF-κB p65 were significantly increased, but IκBα markedly

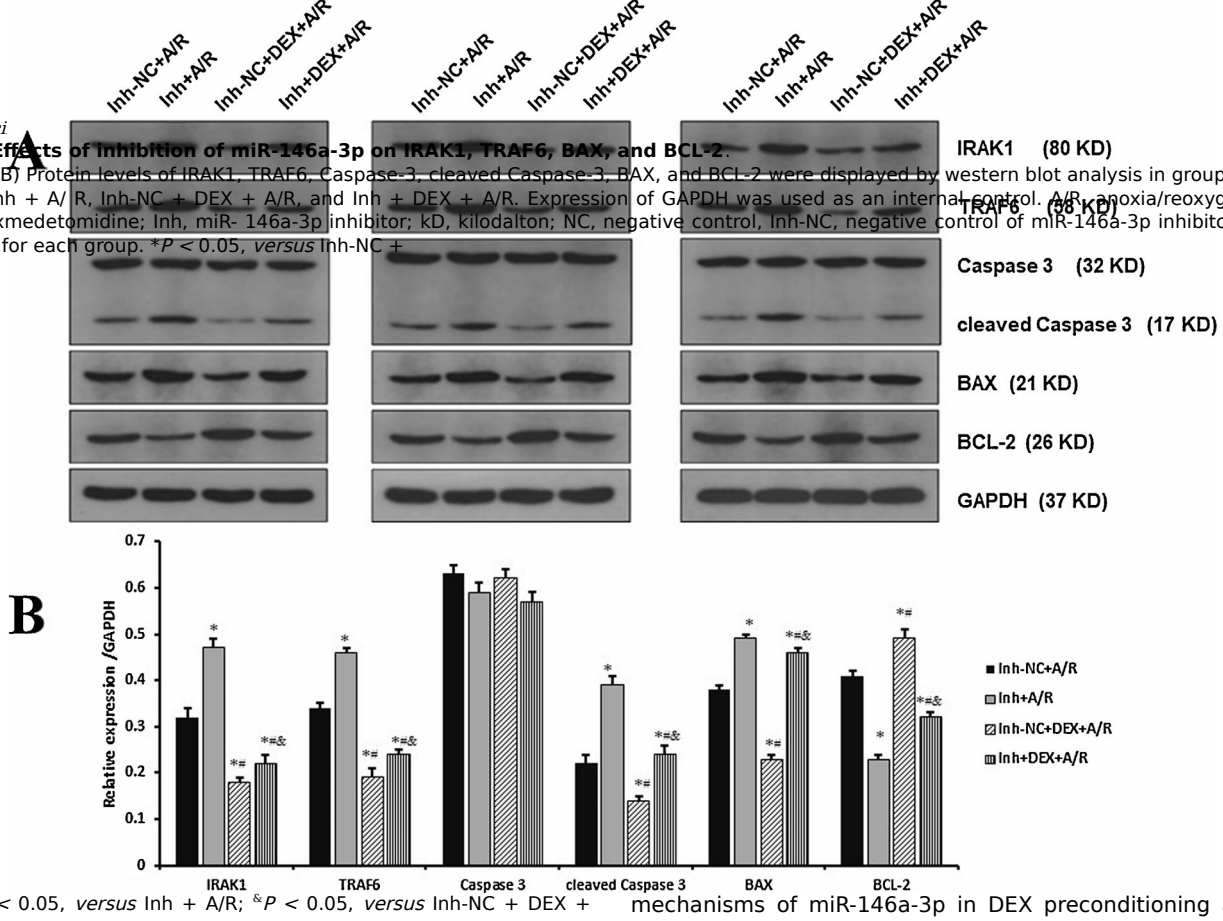

Fig. 8. Effects of inhibition of miR-146a-3p on IRAK1, TRAF6, BAX, and BCL-2.
(A) and (B) Protein levels of IRAK1, TRAF6, Caspase-3, cleaved Caspase-3, BAX, and BCL-2 were displayed by western blot analysis in groups Inh-NC + A/R, Inh + A/ R, Inh-NC + DEX + A/R, and Inh + DEX + A/R. Expression of GAPDH was used as an internal control. A/R, anoxia/reoxygenation; DEX, dexmedetomidine; Inh, miR- 146a-3p inhibitor; kD, kilodalton; NC, negative control, Inh-NC, negative control of miR-146a-3p inhibitor. N = 3 samples for each group. $^{*}P < 0.05$, *versus* Inh-NC + A/R; $^{\#}P < 0.05$, *versus* Inh + A/R; $^{\&}P < 0.05$, *versus* Inh-NC + DEX + A/R.

decreased in H9C2 cells in group A/R compared with group Control. DEX preconditioning reversed the expression levels of p-IκBα, NF-κB p65, p-NF-κB p65, and IκBα in H9C2 cells under A/R. Protein levels of p- IκBα, IκBα, NF-κB p65, and p-NF-κB p65 in Mim + DEX + A/R group were not significantly different from those in Mim-NC + DEX + A/R. Levels of p-IκBα, NF-κB p65, and p-NF-κB p65 were significantly decreased in Mim + siIRAK1 + DEX + A/R or Mim + siTRAF6 + DEX + A/R group compared with Mim + DEX + A/R, but level of IκBα increased (Fig. 9D, E).

3.10. Effects of siIRAK1 or siTRAF6 on ROS emission

Levels of ROS in H9C2 cells were significantly increased in A/R group compared with Control. DEX preconditioning attenuated ROS emission in H9C2 cells under A/R. Levels of ROS in Mim + DEX + A/R group were significantly decreased compared with those in group Mim- NC + DEX + A/R. Levels of ROS were significantly decreased in group
Mim + DEX + A/R compared with those in group A/R or group DEX + A/R. Levels of ROS were significantly decreased further in group Mim + siIRAK1 + DEX + A/R or group Mim + siTRAF6 + DEX + A/R compared with those in group Mim + DEX + A/R or group DEX + A/R (Fig. 10A,
B).

4. Discussion

In this study, myocardial I/R injury was conducted in a rat model. According to profiling of dysregulated miRs on myocardia *in vivo* study and bioinformatic analysis, miR-146a-3p was selected for further study to reveal mechanisms of cardioprotective effects induced by DEX preconditioning. Cellular A/R model was established to explore the effect and mechanisms of miR-146a-3p in DEX preconditioning against myocardial I/R injury. First, we observed that DEX can decrease myocardial infarction size and upregulate expression of miR-146a-3p. Second, expressions of miR-146a-3p were significantly decreased in H9C2 cells under A/R, but significantly increased in H9C2 pretreated with DEX before A/R. Third, overexpression of miR-146a-3p significantly alleviated A/R injury and improved cell viability by inhibiting apoptosis of H9C2 cells. Fourth, downregulation of miR-146a-3p aggravated A/R injury and apoptosis of H9C2 cells. Fifth, DEX preconditioning prevented cardiomyocytes from A/R injury through upregulating miR-146a-3p targeting *IRAK1* and *TRAF6 via* inhibition of NF- κB signaling pathway and ROS emission.

A body of evidence indicates that miRs play important roles in suppressing posttranscriptional genes expression [15,16,18,28]. miRs play important roles in many pathophysiological processes including MI, I/R injury, hypertrophy, arrhythmia, and heart failure [17,20,27,34]. In our previous study, we concluded that miR-665 is involved in cardioprotection induced by DEX in isolated hearts undergoing I/R and in H9C2 cells exposed to H_2O_2 [11]. Our recent study revealed that DEX induces downregulation of miR-208b-3p in rat hearts [35]. Further study indicated that miR-208b-3p/Med13/Wnt/β-catenin axis is implicated in preventing H9C2 from hypoxia/reoxygenation injury [36]. In the present *in vivo* study, we found that miR-146a-3p is upregulated in rat hearts pretreated with DEX before I/R injury, but not in other

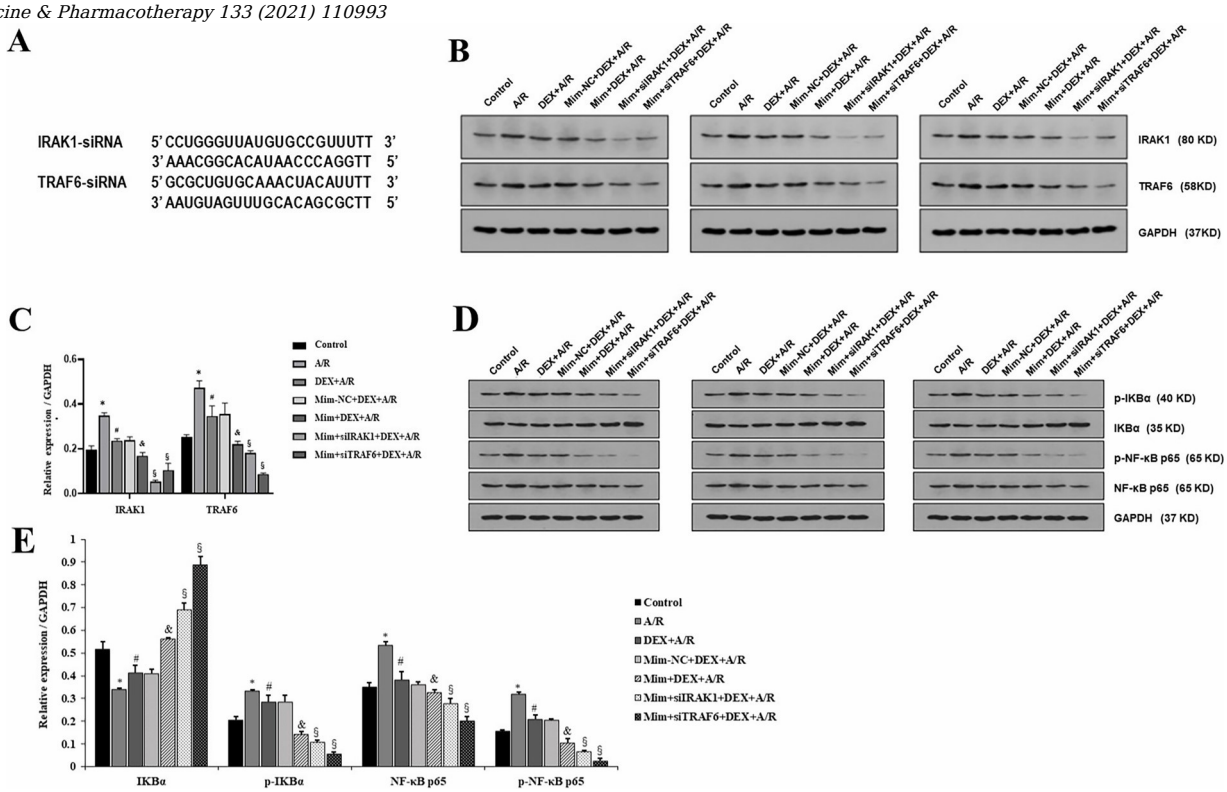

Fig. 9. Effects of siIRAK1 or siTRAF6 on NF-κB pathway.
(A) Sequences of *siIRAK1* or *siTRAF6*. (B) and (C) protein expressions of IRAK1 or TRAF6 were measured by western blot analysis. (D) and (E) protein expressions of IκBα, p-IκBα, NF-κB p65, and p-NF-κB p65 were displayed. Expression of GAPDH was used as an internal control for proteins. A/R, anoxia/reoxygenation; DEX, dexmedetomidine; KD, kilodalton; Mim, miR-146a-3p mimics; Mim-NC, miR-146a-3p mimics negative control; siIRAK1, silencing IRAK1; siTRAF6, silencing TRAF6.
N = 3 samples for each group. $^{*}P < 0.05$, *versus* Control; $^{\#}P < 0.05$, *versus* A/R; $^{\&}P < 0.05$, *versus* DEX + A/R; $^{\S}P < 0.05$, *versus* Mim + DEX + A/R.

experimental models, such as in isolated rat hearts subjected to I/R [11], or in our clinical trial [37]. The reason for the discrepancy may be attributed to the different experimental models we employed. Because the expressions and roles of miRs are context-dependent, which account for differences in regulatory mechanisms of miRs [38,39].

An et al. [28] reported that upregulation of miR-146a alleviates myocardial injury by inhibition of NF-κB activation and inflammatory cytokine production through targeting ErbB4 in LPS-induced sepsis. Likewise, overexpression of miR-146a prevents myocardia from I/R injury *via* targeting IRAK1 and TRAF6 through inhibition of NF-κB activation and inflammatory cytokine production [19]. Exogenous miRNA-146a improves cardiac functions in I/R injury by increasing vascular endothelial growth factor secretion [40]. Infarcted hearts injected with extracellular vesicles from human cardiac progenitor cells, in which miR-210, miR-132, and miR-146a-3p were highly expressed, exhibited decreased cardiomyocyte apoptosis, enhanced angiogenesis, and improved left ventricular ejection fraction [41].These data suggest that miR-146a and miR-146a-3p have anti-apoptotic and cardioprotective effects.

However, Higher levels of miR-146a/b were observed in patients with coronary artery disease [42]. Upregulation of miR-146a was associated with severity of coronary heart disease in patients with subclinical hypothyroidism [43]. Upregulation of miR-146a/b level was related to restenosis and rapid angiographic stenotic progression risk in patients with emergency drug-eluting stent implantation [44]. In a model of post-partum cardiomyopathy, miR-146a-enriched exosomes upregulated miR-146a levels, downregulated miR-146a target genes, and depressed contractile function. Downregulating miR-146a attenuated a post-partum cardiomyopathy [22]. These studies revealed that miR-146a may act as a biomarker of cardiomyocyte damage [45].

The roles of non-coding RNAs (including miR-146a) in physiological and pathological processes depend on different experimental situations. Furthermore, there is a difference between miR-146a and miR-146a-3p in their sequence, so different effects would be induced. As mentioned above, even the same miR could demonstrate opposite effect in different labs due to experimental conditions, *i.e.*, difference in the duration of anoxia and/or reperfusion. Finally, higher expression of miR-146a in patients with coronary heart disease does not necessarily follow that miR-146a is harmful to myocardial cells, and it needs to be pointed out that upregulation of miR-146a following coronary infarction may exert a compensative effect against myocardial injury. Our result indicated that miR-146a-3p plays a role in DEX-induced protection of cardiomyocyte against A/R injury through inhibition of apoptosis.

DEX pretreatment could mimic ischemic preconditioning (an endogenous protective event) and prevent rat hearts from I/R injury [11,46]. In this study, DEX induced myocardial protection by reducing infarction size in the rat hearts subjected to I/R injury.

At the earliest stage of reperfusion after ischemia, cardiomyocyte apoptosis and necrosis account for most of the clinical manifestations [47,48], and inhibition of apoptosis indicates an effective therapeutic strategy against MI and myocardial IRI [48]. The apoptosis assessed by flow cytometry in H9C2 cells was significantly attenuated by pretreatment with DEX. The apoptotic rates of H9C2 cells transfected with

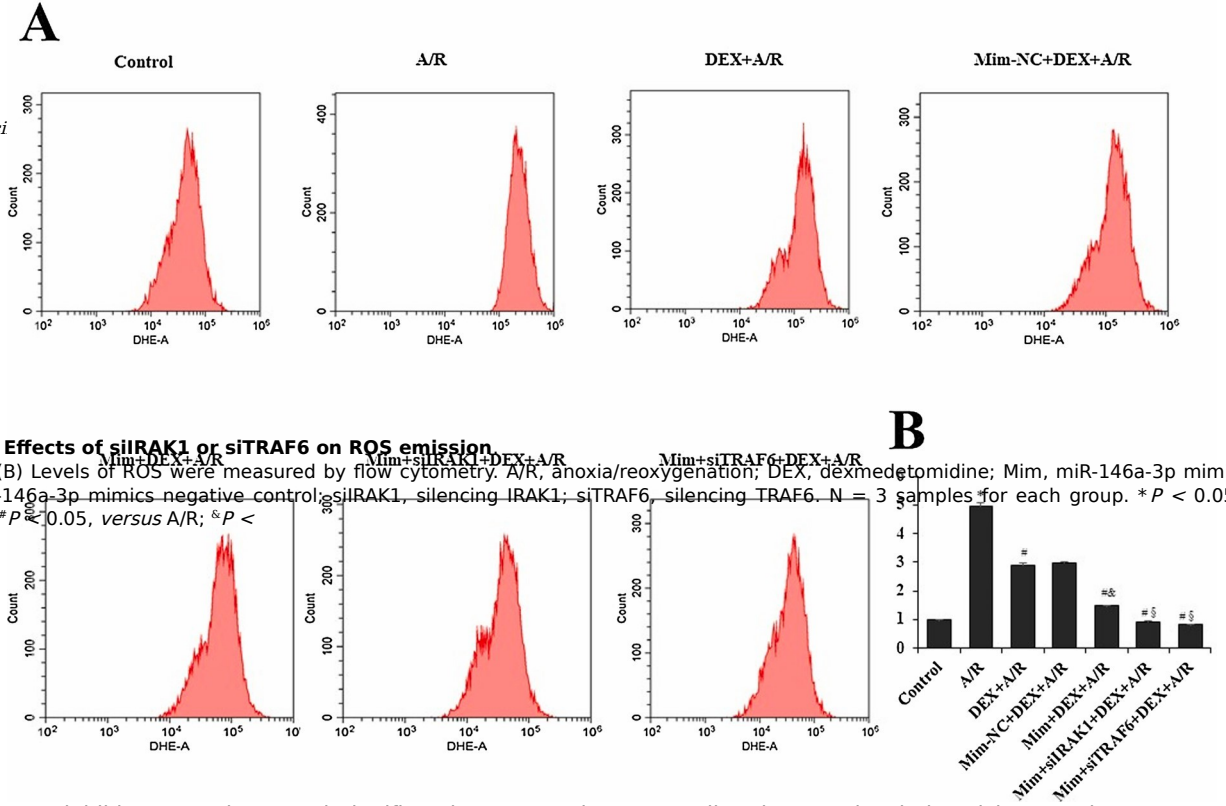

Fig. 10. Effects of siIRAK1 or siTRAF6 on ROS emission.
(A) and (B) Levels of ROS were measured by flow cytometry. A/R, anoxia/reoxygenation; DEX, dexmedetomidine; Mim, miR-146a-3p mimics; Mim-NC, miR-146a-3p mimics negative control; siIRAK1, silencing IRAK1; siTRAF6, silencing TRAF6. N = 3 samples for each group. $^{*}P < 0.05$, *versus* Control; $^{\#}P < 0.05$, *versus* A/R; $^{\&}P < 0.05$, *versus* A/R + DEX; $^{\S}P < 0.05$, *versus* Mim + DEX + A/R.

miR-146a-3p inhibitor were increased significantly compared with those in groups pretreated DEX. This result indicated that miR-146a-3p also played a key role in inhibiting cardiomyocyte apoptosis during DEX-induced cardiomyocyte protection against A/R injury.

miR-146a is an anti-apoptotic miR, and it has been shown to play a role in downregulating IRAK1- and TRAF6-mediated promotion of apoptosis in human dendritic [25] and cervical cancer cells [49]. miR-146a is shown to reduce apoptosis rates in H9C2 cells induced by LPS [28]. In this study, we showed that miR-146a-3p is involved in cardiomyocyte protection by DEX in H9C2 cells under A/R injury. Our results suggested that DEX can protect H9C2 against A/R injury *via* upregulation of miR-146a-3p and downregulation of targets IRAK1 and TRAF6.

With upregulation of miR-146a-3p, protein expressions of IRAK1 and TRAF6 were significantly decreased in H9C2 cells treated with DEX. The anti-apoptotic effect of miR-146a-3p upregulated by DEX in cardiomyocytes can be attributed, at least in part, to the suppression of IRAK1 and TRAF6. This finding suggests that a single molecule may prevent H9C2 cells from A/R injury by a process with multiple pathophysiological components. This may relate to new knowledge of an epigenomic mechanism of myocardial protection induced by DEX pretreatment.

Unlike necrosis in terms of unregulated and uncoordinated pathophysiological mechanisms, apoptosis is a programed cell death process with mechanisms of specific signal transduction [4]. Bcl-2, Bax, and Caspase-3 (cleaved Caspase-3) play crucial roles in cellular apoptosis with complicated mechanisms [50,51]. BCL-2, an anti-apoptotic member of the BCL-2 family, inhibits mitochondrial membrane permeabilization, regulating apoptosome assembly and activation by blocking cytosolic translocation of death amplification factors [52]. Once apoptosis is induced, the downstream effector caspases (including caspase-3) can be activated [53]. The crosstalk of BCL-2, Bax, and cleaved Caspase-3 suggests another apoptotic process in cardiomyocytes. IRAK1 and TRAF6 were involved in miR-146a-3p-mediated protection induced by DEX in H9C2 under A/R injury *in vitro*. Therefore, miR-146a-3p could constitute an active molecule under myocardial disease conditions.

In epithelial vasculature, deletion of TRAF6 leads to loss of nuclear factor kappa B (NF-kB) activity [54]. NF-κB is a transcription factor associated with inflammatory induction and sensitive to redox state in most types of cells [55]. The NF-κB dimer (p65/50) normally exists in inactive cytoplasmic complexes combined with inhibitor of κB alpha (IκBα). Upon stimulation, IκBα is phosphorylated and subjected to degradation, subsequently resulting in dissociation of IκBα/NF-κB complex [29]. NF-κB activation plays a key role in I/R injury, so inhibition of NF-κB may be a potential therapy for I/R injury. The previous study revealed that overexpression of IκBα can protect cardiomyocytes from H_2O_2 induced injury *via* inhibition of NF-κB signaling pathway protein [56]. However, reduction of miR-146a increases NF-kB expression and thus intensifies inflammation and apoptosis in rat hippocampuses [57]. In the current study, protein expressions of IκBα were decreased following A/R, while increased following DEX preconditioning and/or overexpression of miR-146a-3p. Knockdown of IRAK1 or TRAF6 resulted in upregulation of IκBα and downregulation of NF-κB p65, p-NF-κB p65, and p-IκBα in H9C2 cells. Our results indicated that A/R induced H9C2 injury is caused partly by downregulation of miR-146a-3p targeting IRAK1 and TRAF6 and activation of NF-κB signaling pathway and that the injury was alleviated through DEX preconditioning *via* reversing these changes. Therefore, targeting the IRAK1/NF-κB or TRAF6/NF-κB signaling pathway may be the promising therapeutic strategies against myocardial injury.

According to our profiling of miRs, some of them are altered by DEX, and each one of them affects numerous targeting genes. That a single interference with one miR completely blocks the protection may be overstated. A novel miR-146b/TRAF6 axis may drive cardiac inflammation, fibrosis, and dysfunction [58]. Therefore, a network and crosstalk of some miRs should be taken into consideration in future studies [17].

In the present study, we have not checked any potential changes in IRAK1, TRAF6 and apoptosis execution in

myocardia *in vivo*. Using miR- 146a-3p as a possible therapeutic agent for myocardial IRI has not been studied, so this is a limitation of our *in vivo* study. However, the emerging data denote future applications of non-coding RNA-based strategies (such as a specific miR-146a from exosomes [41]) in small molecule therapy and biologic therapy [59].

The levels of reactive oxygen species (ROS) play an important role in ischemia/reperfusion injury. It is documented that reducing ROS generation can alleviate myocardial IRI and H9C2 cell injury caused by A/R [60]. Some miRs are involved in regulation of ROS mediated myocardial IRI and function as biomarkers of MI [61]. miR-146a plays an important role in regulating oxidative stress [62]. In the present study, we also found that upregulation of miR-146a-3p by miR-146a-3p-mimics or DEX preconditioning reduced ROS emission. Knockdown of the target genes (IRAK1 and TRAF6) also downregulated ROS levels. So our findings suggest that DEX induced differential expressions of miR-146a-3p and the target genes play an important role in regulation of ROS, which may be involved in DEX exerted cardioprotection along with inhibition of NF-κB.

5. Conclusions

These findings suggest that miR-146a-3p targeting *IRAK1* and *TRAF6* decreases H9C2 injury under A/R partly *via* inhibition of NF-κB signaling pathway and ROS emission. Our results indicate that DEX preconditioning induced upregulation of miR-146a-3p targeting IRAK1/ NF-κB or TRAF6/NF-κB signaling pathway and decreasing ROS emission may be a promising therapeutic and preventive strategy for myocardial IRI.

Funding

This work was supported by National Natural Science Foundation of China (81860050 & 81460044), Yunnan Health Training Project of High Levels Talents (L-2018007), Yunnan Provincial Science and Technology Department (2017FE468-039), Health and Family Planning Commission of Yunnan Province (2018NS0126), Program for Innovative Research Team of Kunming Medical University (CXTD201802), and Yunnan Provincial Ten Thousand-Talent Program-Famous Doctor (YNWR-MY- 2018-043).

Declaration of Competing Interest

The authors report no declarations of interest.

References

[1] E.J. Benjamin, S.S. Virani, C.W. Callaway, A.M. Chamberlain, A.R. Chang, S. Cheng, S.E. Chiuve, M. Cushman, F.N. Delling, R. Deo, S.D. de Ferranti, J.
F. Ferguson, M. Fornage, C. Gillespie, C.R. Isasi, M.C. Jimenez, L.C. Jordan, S.
E. Judd, D. Lackland, J.H. Lichtman, L. Lisabeth, S. Liu, C.T. Longenecker, P.
L. Lutsey, J.S. Mackey, D.B. Matchar, K. Matsushita, M.E. Mussolino, K. Nasir,
M. O'Flaherty, L.P. Palaniappan, A. Pandey, D.K. Pandey, M.J. Reeves, M. D. Ritchey, C.J. Rodriguez, G.A. Roth, W.D. Rosamond, U.K.A. Sampson, G.
M. Satou, S.H. Shah, N.L. Spartano, D.L. Tirschwell, C.W. Tsao, J.H. Voeks, J.
Z. Willey, J.T. Wilkins, J.H. Wu, H.M. Alger, S.S. Wong, P. Muntner, Heart disease and stroke statistics-2018 update: a report from the American Heart Association, Circulation 137 (12) (2018) e67–e492, https://doi.org/10.1161/ cir.0000000000000558.

[2] F. Montecucco, F. Carbone, T.H. Schindler, Pathophysiology of ST-segment elevation myocardial infarction: novel mechanisms and treatments, Eur. Heart J.
37 (16) (2016) 1268–1283, https://doi.org/10.1093/eurheartj/ehv592.

[3] S. Windecker, J.J. Bax, A. Myat, G.W. Stone, M.S. Marber, Future treatment strategies in ST-segment elevation myocardial infarction, Lancet 382 (9892) (2013) 644–657, https://doi.org/10.1016/s0140-6736(13)61452-x.

[4] B. Ibanez, G. Heusch, M. Ovize, F. Van de Werf, Evolving therapies for myocardial ischemia/reperfusion injury, J. Am. Coll. Cardiol. 65 (14) (2015) 1454–1471, https://doi.org/10.1016/j.jacc.2015.02.032.

[5] D.A. Jones, K.S. Rathod, A. Williamson, D. Harrington, M. Andiapen, S. van Eijl, M. Westwood, S. Antoniou, R.J. Schilling, A. Ahluwalia, A. Mathur, The effect of intracoronary sodium nitrite on the burden of ventricular arrhythmias following primary percutaneous coronary intervention for acute myocardial infarction, Int. J. Cardiol. 266 (2018) 1–6, https://doi.org/10.1016/j.ijcard.2018.01.029.

[6] R.J. Alleman, A.M. Tsang, T.E. Ryan, D.J. Patteson, J.M. McClung, E. E. Spangenburg, S.R. Shaikh, P.D. Neufer, D.A. Brown, Exercise-induced protection against reperfusion arrhythmia involves stabilization of mitochondrial energetics, Am. J. Physiol. Heart Circ. Physiol. 310 (10) (2016) H1360–1370, https://doi.org/ 10.1152/ajpheart.00858.2015.

[7] B.L. Udeh, J.E. Dalton, J.S. Hata, C.I. Udeh, D.I. Sessler, Economic trends from 2003 to 2010 for perioperative myocardial infarction: a retrospective, cohort study, Anesthesiology 121 (1) (2014) 36–45, https://doi.org/10.1097/ aln.0000000000000233.

[8] G.M. Keating, Dexmedetomidine: a review of its use for sedation in the intensive care setting, Drugs 75 (10) (2015) 1119–1130, https://doi.org/10.1007/s40265- 015-0419-5.

[9] F. Behmenburg, E. Pickert, A. Mathes, A. Heinen, M.W. Hollmann, R. Huhn, M. M. Berger, The cardioprotective effect of dexmedetomidine in rats is dose- dependent and mediated by BKCa channels, J. Cardiovasc. Pharmacol. 69 (4) (2017) 228–235, https://doi.org/10.1097/fjc.0000000000000466.

[10] J.A. Riquelme, F. Westermeier, A.R. Hall, J.M. Vicencio, Z. Pedrozo, M. Ibacache, B. Fuenzalida, L. Sobrevia, S.M. Davidson, D.M. Yellon, G. Sanchez, S. Lavandero, Dexmedetomidine protects the heart against ischemia-reperfusion injury by an endothelial eNOS/NO dependent mechanism, Pharmacol. Res. 103 (2016) 318–327, https://doi.org/10.1016/j.phrs.2015.11.004.

[11] J. Yu, W. Yang, W. Wang, Z. Wang, Y. Pu, H. Chen, F. Wang, J. Qian, Involvement of miR-665 in protection effect of dexmedetomidine against Oxidative Stress Injury in myocardial cells via CB2 and CK1, Biomed. Pharmacother. 115 (2019), 108894, https://doi.org/10.1016/j.biopha.2019.108894.

[12] R.D. Sanders, J. Xu, Y. Shu, A. Januszewski, S. Halder, A. Fidalgo, P. Sun, M. Hossain, D. Ma, M. Maze, Dexmedetomidine attenuates isoflurane-induced neurocognitive impairment in neonatal rats, Anesthesiology 110 (5) (2009) 1077–1085, https://doi.org/10.1097/ALN.0b013e31819daedd.

[13] J.F. Perez-Zoghbi, W. Zhu, M.R. Grafe, A.M. Brambrink, Dexmedetomidine- mediated neuroprotection against sevoflurane-induced neurotoxicity extends to several brain regions in neonatal rats, Br. J. Anaesth. 119 (3) (2017) 506–516, https://doi.org/10.1093/bja/aex222.

[14] J. Cui, H. Zhao, B. Yi, J. Zeng, K. Lu, D. Ma, Dexmedetomidine attenuates bilirubin- induced lung alveolar epithelial cell death in vitro and in vivo, Crit. Care Med. 43 (9) (2015) e356–368, https://doi.org/10.1097/ccm.0000000000001035.

[15] D.P. Bartel, Metazoan microRNAs, Cell 173 (1) (2018) 20–51, https://doi.org/
10.1016/j.cell.2018.03.006.

[16] D.P. Bartel, MicroRNAs: target recognition and regulatory functions, Cell 136 (2) (2009) 215–233, https://doi.org/10.1016/j.cell.2009.01.002.

[17] L. He, Y. Chen, S. Hao, J. Qian, Uncovering novel landscape of cardiovascular diseases and therapeutic targets for cardioprotection via long noncoding RNA- miRNA-mRNA axes, Epigenomics 10 (5) (2018) 661–671, https://doi.org/ 10.2217/epi-2017-0176.

[18] M. Arif, R. Pandey, P. Alam, S. Jiang, S. Sadayappan, A. Paul, R.P.H. Ahmed, MicroRNA-210-mediated proliferation, survival, and angiogenesis promote cardiac repair post myocardial infarction in rodents, J. Mol. Med (Berl) 95 (12) (2017) 1369–1385, https://doi.org/10.1007/s00109-017-1591-8.

[19] X. Wang, T. Ha, L. Liu, J. Zou, X. Zhang, J. Kalbfleisch, X. Gao, D. Williams, C. Li, Increased expression of microRNA-146a decreases myocardial ischaemia/ reperfusion injury, Cardiovasc. Res. 97 (3) (2013) 432–442, https://doi.org/ 10.1093/cvr/cvs356.

[20] X. Liu, Y. Dong, S. Chen, G. Zhang, M. Zhang, Y. Gong, X. Li, Circulating microRNA-146a and microRNA-21 predict left ventricular remodeling after ST- elevation myocardial infarction, Cardiology 132 (4) (2015) 233–241, https://doi. org/10.1159/000437090.

[21] A.B. Arroyo, A.M. de Los Reyes-Garcia, J.M. Rivera-Caravaca, P. Valledor, N. Garcia-Barbera, V. Roldan, V. Vicente, C. Martinez, R. Gonzalez-

Conejero, MiR- 146a regulates neutrophil extracellular trap formation that predicts adverse cardiovascular events in patients with atrial fibrillation, Arterioscler. Thromb. Vasc. Biol. 38 (4) (2018) 892–902, https://doi.org/10.1161/atvbaha.117.310597.
[22] J. Halkein, S.P. Tabruyn, M. Ricke-Hoch, A. Haghikia, N.Q. Nguyen, M. Scherr, K. Castermans, L. Malvaux, V. Lambert, M. Thiry, K. Sliwa, A. Noel, J.A. Martial, D. Hilfiker-Kleiner, I. Struman, MicroRNA-146a is a therapeutic target and biomarker for peripartum cardiomyopathy, J. Clin. Invest. 123 (5) (2013) 2143–2154, https://doi.org/10.1172/jci64365.
[23] Z. Zeng, H. Gong, Y. Li, K. Jie, C. Ding, Q. Shao, F. Liu, Y. Zhan, C. Nie, W. Zhu, K. Qian, Upregulation of miR-146a contributes to the suppression of inflammatory responses in LPS-induced acute lung injury, Exp. Lung Res. 39 (7) (2013) 275–282, https://doi.org/10.3109/01902148.2013.808285.
[24] X. Chen, M. Xie, D. Liu, K. Shi, Downregulation of microRNA146a inhibits ovarian granulosa cell apoptosis by simultaneously targeting interleukin1 receptorassociated kinase and tumor necrosis factor receptorassociated factor 6, Mol. Med. Rep. 12 (4) (2015) 5155–5162, https://doi.org/10.3892/ mmr.2015.4036.
[25] H. Park, X. Huang, C. Lu, M.S. Cairo, X. Zhou, MicroRNA-146a and microRNA- 146b regulate human dendritic cell apoptosis and cytokine production by targeting TRAF6 and IRAK1 proteins, J. Biol. Chem. 290 (5) (2015) 2831–2841, https://doi. org/10.1074/jbc.M114.591420.
[26] J. Hou, P. Wang, L. Lin, X. Liu, F. Ma, H. An, Z. Wang, X. Cao, MicroRNA-146a feedback inhibits RIG-I-dependent type I IFN production in macrophages by targeting TRAF6, IRAK1, and IRAK2, J. Immunol. 183 (3) (2009) 2150–2158, https://doi.org/10.4049/jimmunol.0900707.
[27] M. Gao, X. Wang, X. Zhang, T. Ha, H. Ma, L. Liu, J.H. Kalbfleisch, X. Gao, R.L. Kao, D.L. Williams, C. Li, Attenuation of cardiac dysfunction in polymicrobial sepsis by microRNA-146a is mediated via targeting of IRAK1 and TRAF6 expression,
J. Immunol. 195 (2) (2015) 672–682, https://doi.org/10.4049/jimmunol.1403155.
[28] R. An, J. Feng, C. Xi, J. Xu, L. Sun, miR-146a attenuates sepsis-induced myocardial dysfunction by suppressing IRAK1 and TRAF6 via targeting ErbB4 expression, Oxid. Med. Cell. Longev. 2018 (2018), 7163057, https://doi.org/10.1155/2018/ 7163057.
[29] A. Oeckinghaus, S. Ghosh, The NF-kappaB family of transcription factors and its regulation, Cold Spring Harbor Perspect. Biol. 1 (2009) 1–14, https://doi.org/ 10.1101/cshprespect.a000034.
[30] W. Zhang, M. Shao, X. He, B. Wang, Y. Li, X. Guo, Overexpression of microRNA- 146 protects against oxygen-glucose deprivation/recovery-induced cardiomyocyte apoptosis by inhibiting the NF-κB/TNF-α signaling pathway, Mol. Med. Rep. 17 (1) (2018) 1913–1918, https://doi.org/10.3892/mmr.2017.8073.
[31] H. Parlakpinar, E. Sahna, A. Acet, B. Mizrak, A. Polat, Protective effect of caffeic acid phenethyl ester (CAPE) on myocardial ischemia-reperfusion-induced apoptotic cell death, Toxicology 209 (1) (2005) 1–14, https://doi.org/10.1016/j. tox.2004.10.017.
[32] L. He, S. Hao, Y. Wang, W. Yang, L. Liu, H. Chen, J. Qian, Dexmedetomidine preconditioning attenuates ischemia/reperfusion injury in isolated rat hearts with endothelial dysfunction, Biomed. Pharmacother. 114 (2019), 108837, https://doi.org/10.1016/j.biopha.2019.108837.
[33] F. Cheng, W. Yuan, M. Cao, R. Chen, X. Wu, J. Yan, Cyclophilin A protects cardiomyocytes against hypoxia/reoxygenation-induced apoptosis via the AKT/ Nox2 pathway, Oxid. Med. Cell. Longev. 2019 (2019), 2717986, https://doi.org/ 10.1155/2019/2717986.
[34] J.G. Oh, S. Watanabe, A. Lee, P.A. Gorski, P. Lee, D. Jeong, L. Liang, Y. Liang, A. Baccarini, S. Sahoo, B.D. Brown, R.J. Hajjar, C. Kho, miR-146a suppresses
SUMO1 expression and induces cardiac dysfunction in maladaptive hypertrophy,
J. Cell. Biochem. 123 (6) (2018) 673–685, https://doi.org/10.1002/jcb.27731
10.1161/circresaha.118.312751.
[35] L. Wang, S. Tang, Z. Wang, H. Chen, S.S. Rajcha, J. Qian, The administration of dexmedetomidine changes microRNA expression profiling of rat hearts, Biomed. Pharmacother. 120 (2019), https://doi.org/10.1016/j.biopha.2019.109463, 109463-109463.
[36] Z. Wang, Y. Yang, W. Xiong, R. Zhou, N. Song, L. Liu, J. Qian, Dexmedetomidine protects H9C2 against hypoxia/reoxygenation injury through miR-208b-3p/ Med13/Wnt signaling pathway axis, Biomed. Pharmacother. 125 (2020), 110001, https://doi.org/10.1016/j.biopha.2020.110001.
[37] X. Yang, H. Chen, Y. Chen, Y. Birnbaum, R. Liang, Y. Ye, J. Qian, Circulating miRNA expression profiling and target prediction in patients receiving dexmedetomidine, Cell. Physiol. Biochem. 50 (2) (2018) 552–568, https://doi.org/ 10.1159/000494168.
[38] J. Koo, J. Zhang, S. Chaterji, Tiresias: context-sensitive approach to decipher the presence and strength of microRNA regulatory interactions, Theranostics 8 (1) (2018) 277–291, https://doi.org/10.7150/thno.22065.
[39] M. Vitiello, A. Tuccoli, R. D'Aurizio, S. Sarti, L. Giannecchini, S. Lubrano, A. Marranci, M. Evangelista, S. Peppicelli, C. Ippolito, I. Barravecchia, E. Guzzolino, V. Montagnani, M. Gowen, E. Mercoledi, A. Mercatanti, L. Comelli,
S. Gurrieri, L.W. Wu, O. Ope, K. Flaherty, G.M. Boland, M.R. Hammond, L. Kwong,
M. Chiariello, B. Stecca, G. Zhang, A. Salvetti, D. Angeloni, L. Pitto, L. Calorini, G. Chiorino, M. Pellegrini, M. Herlyn, I. Osman, L. Poliseno, Context-dependent miR-204 and miR-211 affect the biological properties of amelanotic and melanotic melanoma cells, Oncotarget 8 (15) (2017) 25395–25417, https://doi.org/ 10.18632/oncotarget.15915.
[40] H.-H. Seo, S.-Y. Lee, C.Y. Lee, R. Kim, P. Kim, S. Oh, H. Lee, M.Y. Lee, J. Kim, L.
K. Kim, K.-C. Hwang, W. Chang, Exogenous miRNA-146a enhances the therapeutic efficacy of human mesenchymal stem cells by increasing vascular endothelial growth factor secretion in the ischemia/reperfusion-injured heart, J. Vasc. Res. 54 (2) (2017) 100–108, https://doi.org/10.1159/000461596.
[41] L. Barile, V. Lionetti, E. Cervio, M. Matteucci, M. Gherghiceanu, L.M. Popescu, T. Torre, F. Siclari, T. Moccetti, G. Vassalli, Extracellular vesicles from human cardiac progenitor cells inhibit cardiomyocyte apoptosis and improve cardiac function after myocardial infarction, Cardiovasc. Res. 103 (4) (2014) 530–541, https://doi.org/10.1093/cvr/cvu167.
[42] Y. Takahashi, M. Satoh, Y. Minami, T. Tabuchi, T. Itoh, M. Nakamura, Expression of miR-146a/b is associated with the Toll-like receptor 4 signal in coronary artery disease: effect of renin-angiotensin system blockade and statins on miRNA-146a/b and Toll-like receptor 4 levels, Clin. Sci. (Lond.) 119 (9) (2010) 395–405, https://doi.org/10.1042/cs20100003.
[43] X. Quan, Y. Ji, C. Zhang, X. Guo, Y. Zhang, S. Jia, W. Ma, Y. Fan, C. Wang, Circulating miR-146a may be a potential biomarker of coronary heart disease in patients with subclinical hypothyroidism, Cell. Physiol. Biochem. 45 (1) (2018) 226–236, https://doi.org/10.1159/000486769.
[44] H. Zhang, Q. Zhang, Y. Liu, T. Xue, miR-146a and miR-146b predict increased restenosis and rapid angiographic stenotic progression risk in coronary heart disease patients who underwent percutaneous coronary intervention, Ir. J. Med.
Sci. 189 (2) (2020) 467–474, https://doi.org/10.1007/s11845-019-02101-9.
[45] G.Z. Yu, S. Reilly, A.J. Lewandowski, C.Y.L. Aye, L.J. Simpson, L. Newton, E.
F. Davis, S.J. Zhu, W.R. Fox, A. Goel, H. Watkins, K.M. Channon, S.M. Watt, T. Kyriakou, P. Leeson, Neonatal micro-RNA profile determines endothelial function in offspring of hypertensive pregnancies, Hypertension 72 (4) (2018) 937–945, https://doi.org/10.1161/hypertensionaha.118.11343.
[46] J. Dong, X. Guo, S. Yang, L. Li, The effects of dexmedetomidine preconditioning on aged rat heart of ischaemia reperfusion injury, Res. Vet. Sci. 114 (2017) 489–492, https://doi.org/10.1016/j.rvsc.2017.09.028.
[47] G.W. Reed, J.E. Rossi, C.P. Cannon, Acute myocardial infarction, Lancet 389 (10065) (2017) 197–210, https://doi.org/10.1016/s0140-6736(16)30677-8.
[48] D.J. Hausenloy, D.M. Yellon, Myocardial ischemia-reperfusion injury: a neglected therapeutic target, J. Clin. Invest. 123 (1) (2013) 92–100, https://doi.org/ 10.1172/jci62874.
[49] Q. Hu, J. Song, B. Ding, Y. Cui, J. Liang, S. Han, miR-146a promotes cervical cancer cell viability via targeting IRAK1 and TRAF6, Oncol. Rep. 39 (6) (2018) 3015–3024, https://doi.org/10.3892/or.2018.6391.
[50] R. Lakshmi Sundaram, H.R. Vasanthi, Dalspinin isolated from Spermacoce hispida (Linn.) protects H9c2 cardiomyocytes from hypoxic injury by modulating oxidative stress and apoptosis, J. Ethnopharmacol. 241 (2019), 111962, https://doi.org/ 10.1016/j.jep.2019.111962.
[51] I. Dolka, M. Krol, R. Sapierzynski, Evaluation of apoptosis-associated protein (Bcl- 2, Bax, cleaved caspase-3 and p53) expression in canine mammary tumors: an immunohistochemical and prognostic study, Res. Vet. Sci. 105 (2016) 124–133, https://doi.org/10.1016/j.rvsc.2016.02.004.
[52] S.O. Pohl, M. Agostino, A. Dharmarajan, S. Pervaiz, Cross talk between cellular redox state and the antiapoptotic protein Bcl-2, Antioxid. Redox Signal. 29 (13) (2018) 1215–1236, https://doi.org/10.1089/ars.2017.7414.
[53] Y. Lu, X. Gao, R. Wang, J. Sun, B. Guo, R. Wei, Y. Jia, Adiponectin inhibits proliferation of vascular endothelial cells induced by Ox-LDL by promoting dephosphorylation of Caveolin-1 and depolymerization of eNOS and up-regulating release of NO, Int. Immunopharmacol. 73 (2019) 424–434, https://doi.org/ 10.1016/j.intimp.2019.05.017.
[54] K.M. Dickson, A.L. Bhakar, P.A. Barker, TRAF6-dependent NF-kB transcriptional activity during mouse development, Dev. Dyn. 231 (1) (2004) 122–127, https:// doi.org/10.1002/dvdy.20110.
[55] H. Sies, C. Berndt, D.P. Jones, Oxidative stress, Annu. Rev. Biochem. 86 (2017) 715–748, https://doi.org/10.1146/annurev-biochem-061516-045037.
[56] M. Han, X.C. Chen, M.H. Sun, M.T. Gai, Y.N. Yang, X.M. Gao, X. Ma, B.D. Chen, Y. T. Ma, Overexpression of IκBα in cardiomyocytes alleviates hydrogen peroxide- induced apoptosis and autophagy by inhibiting NF-

κB activation, Lipids Health Dis. 19 (1) (2020) 150, https://doi.org/10.1186/s12944-020-01327-2.
[57] F. Habibi, F. Ghadiri Soufi, R. Ghiasi, A.M. Khamaneh, M.R. Alipour, Alteration in inflammation-related miR-146a expression in NF-KB Signaling pathway in diabetic rat hippocampus, Adv. Pharm. Bull. 6 (1) (2016) 99–103, https://doi.org/ 10.15171/apb.2016.015.
[58] P. Chouvarine, E. Legchenko, J. Geldner, C. Riehle, G. Hansmann, Hypoxia drives cardiac miRNAs and inflammation in the right and left ventricle, J. Mol. Med. (Berl) 97 (10) (2019) 1427–1438, https://doi.org/10.1007/s00109-019-01817-6.
[59] R.S. Gangwar, S. Rajagopalan, R. Natarajan, J.A. Deiuliis, Noncoding RNAs in cardiovascular disease: pathological relevance and emerging role as biomarkers and therapeutics, Am. J. Hypertens. 31 (2) (2018) 150–165, https://doi.org/ 10.1093/ajh/hpx197.
[60] D. Li, X. Wang, Q. Huang, S. Li, Y. Zhou, Z. Li, Cardioprotection of CAPE-oNO(2) against myocardial ischemia/reperfusion induced ROS generation via regulating the SIRT1/eNOS/NF-κB pathway in vivo and in vitro, Redox Biol. 15 (2018) 62–73, https://doi.org/10.1016/j.redox.2017.11.023.
[61] T. Carbonell, A.V. Gomes, MicroRNAs in the regulation of cellular redox status and its implications in myocardial ischemia-reperfusion injury, Redox Biol. 36 (2020), 101607, https://doi.org/10.1016/j.redox.2020.101607.
[62] Y.G. Zhang, Y. Song, X.L. Guo, R.Y. Miao, Y.Q. Fu, C.F. Miao, C. Zhang, Exosomes derived from oxLDL-stimulated macrophages induce neutrophil extracellular traps to drive atherosclerosis, Cell Cycle 18 (20) (2019) 2674–2684, https://doi.org/ 10.1080/15384101.2019.1654797.